Solid State Phenomena
ISSN: 1662-9779, Vol. 344, pp 29-33
doi:10.4028/p-q6725d

Submitted: 2022-09-04
Revised: 2022-11-25
Accepted: 2022-11-29
Online: 2023-06-06

Study of GHz-Burst Femtosecond Laser Micro-Punching of 4H-SiC Wafers

Hanan Mir[1,2,a*], Fabian Meyer[1,b], Andreas A. Brand[1,c], Katrin Dulitz[1,2,3,d], and Jan-Frederik Nekarda[1,e]

[1]Fraunhofer Institute for Solar Energy Systems ISE, Heidenhofstr. 2, 79110 Freiburg, Germany

[2]Institute of Physics, University of Freiburg, Hermann-Herder-Str. 3, 79104 Freiburg, Germany

[3]Present address: Institut für Ionenphysik und Angewandte Physik, Universität Innsbruck, 6020 Innsbruck, Austria

[a]hanan.mir@ise.fraunhofer.de, [b]fabian.meyer@ise.fraunhofer.de, [c]andreas.brand@ise.fraunhofer.de, [d]katrin.erath-dulitz@uibk.ac.at, [e]jan.nekarda@ise.fraunhofer.de

Keywords: GHz Burst, Ultrashort Laser Pulses, Laser Processing, SiC, Laser Ablation

Abstract. The micromachining of silicon carbide using femtosecond laser pulses is becoming an important field of research. High-repetition-rate sub-pulse trains, so-called pulse bursts, are a particularly promising route towards completely new process regimes. We report on the results of micro-punching n-type 4H-silicon carbide wafers using GHz pulse burst in order to systematically investigate the influence of the temporal energy distribution on laser processing. Pulse-burst experiments are performed at a laser wavelength of $\lambda = 1030$ nm using a single GHz burst containing a varying number of pulses and then compared with standard single femtosecond pulse exposures. The pulse energy is swept across the ablation threshold. For each set of parameters, the micromachining efficiency is evaluated in terms of ablation efficiency and burr characteristics. Scanning electron micrographs provide qualitative information about the machining quality. The characteristics of the laser modification are discussed in relation to an increase in the number of pulses in a burst envelope and to an increase in pulse energy. We observe that, compared to a single pulse, a GHz burst comprised of 10 lower-energy pulses leads to an increase in the ablation rate by a factor of ≤ 10.

Introduction

Laser-based additive and subtractive micromachining is becoming indispensable for the development of a wide range of silicon carbide (SiC)-based semiconductor devices [1]. A bottleneck for laser-assisted micromaching is related to heating and subsequent parasitic damage of the material. Ultrashort pulse (USP) lasers with pulse durations in the femtosecond (fs) regime have remedied this problem along with improved machining precision. However, the full exploitation of USP lasers in terms of high pulse energy and high pulse repetition rate still leads to a high thermal budget [2].

GHz bursts have been shown to minimize these undesirable thermal effects, to improve the ablation efficiency and to lower the threshold of modification for metals and semiconductors including copper and silicon [[3]–[5]. While fs GHz burst processing has been widely studied for metal micromachining [5], [6], its use in wide-bandgap semiconductor micromachining has not been fully evaluated yet. With regard to SiC, only few results are reported, mainly focusing on line-scribing and large-area ablation [7], [8]. SiC micromachining requires a higher thermal load compared to other semiconductor materials. Therefore, the use of GHz bursts may be ideal for SiC laser micromachining. To investigate the influence of the temporal energy redistribution for tuning laser processing, we report on results of micro-punching n-type 4H-SiC wafers with a single GHz burst containing a fixed number of laser pulses. The micromachining efficiency of each processing parameter is evaluated quantitatively in terms of ablation efficiency and burr characteristics. The qualitative analysis of the lasered spots is done using scanning electron microscopy (SEM).

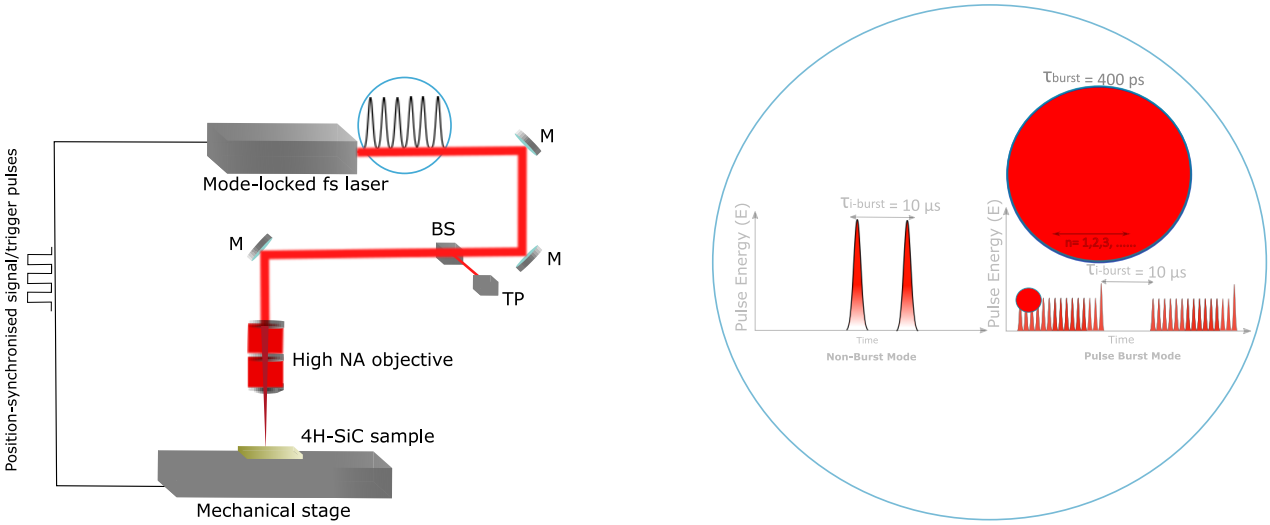

Fig. 1: (a) Schematic drawing of the optical setup. Abbreviations: mirror (M), attenuating beamsplitter (BS), thermopile (TP). (b) Graphical illustration of the difference between the laser processing in non-burst mode (left) and in pulse-burst mode (right).

Experimental Setup

Optical setup. Experiments are done with a commercial fs laser system (Light Conversion Carbide CB3-40W) at a wavelength of λ = 1030 nm and a pulse duration of $\tau \approx 250$ fs. The laser pulse burst mode (PBM) with an intra-burst pulse period $\tau_{\text{burst}} = 400$ ps (corresponding to a frequency of 2.5 GHz) and an inter-burst period $\tau_{\text{i-burst}} = 10\,\mu$s (100 kHz) is used for the present study (cf. Fig. 1(b)). The latter is not relevant for our study, since only single bursts are used here. The optical setup is shown in Fig. 1(a). A benchtop XYZ mechanical stage is used to move the sample and to generate position-synchronised trigger signals to fire single bursts. A high numerical aperture (NA) objective lens with NA = 0.4 is used to focus the laser beam, resulting in a beam waist $\omega_0 = 1.6\,\mu$m. The energies of individual bursts are measured with a high speed thermal sensor (Laserpoint Blink HS).
Parameters for laser processing. A 6-inch 4H-SiC wafer is diced into 15 × 15 mm^2 snippets using a diamond wire saw. For the experiments described here, the spots are lasered on different snippets across the wafer to account for material inhomogeneity which is quite pronounced in 4H-SiC wafers.

In the following, a description of the laser parameters which are varied to study the PBM is provided:
(i) *Pulse fluence*. For a Gaussian laser beam, the pulse fluence Φ_0 is given as

$$\Phi_0 = \frac{2E_{\text{p}}}{\pi\omega_0^2}, \qquad [\text{Jcm}^{-2}] \quad (1)$$

where E_{p} is the pulse energy of each individual pulse in a burst and ω_0 is the beam waist.
(ii) *Number of pulses in a burst packet* The number of pulses in a burst packet n is varied from $n = 1$ (non-burst mode, NBM), to $n = 10$ (pulse-burst mode, PBM). A graphical illustration of the difference between the laser processing in non-burst mode and in pulse-burst mode is shown in Fig. 1(b).
The total burst energy E_{burst} is then given as

$$E_{\text{burst}} = nE_{\text{p}} \qquad [\mu\text{J}] \quad (2)$$

In NBM, the values of $E_{\text{burst}} = E_{\text{p}}$ are varied from 1.7 μJ to 12 μJ. It is important to note that the objective of this work is to study the case in which $E_{\text{p}} << E_{\text{burst}}$.
The ablated spots are then analysed using a confocal profiler (Sensofar PLu S Neox) to obtain the ablation efficiency η which is defined here as the total ablated volume ΔV per pulse:

$$\eta = \Delta V / E_{\text{p}} \qquad [\mu\text{m}^3\mu\text{J}^{-1}] \quad (3)$$

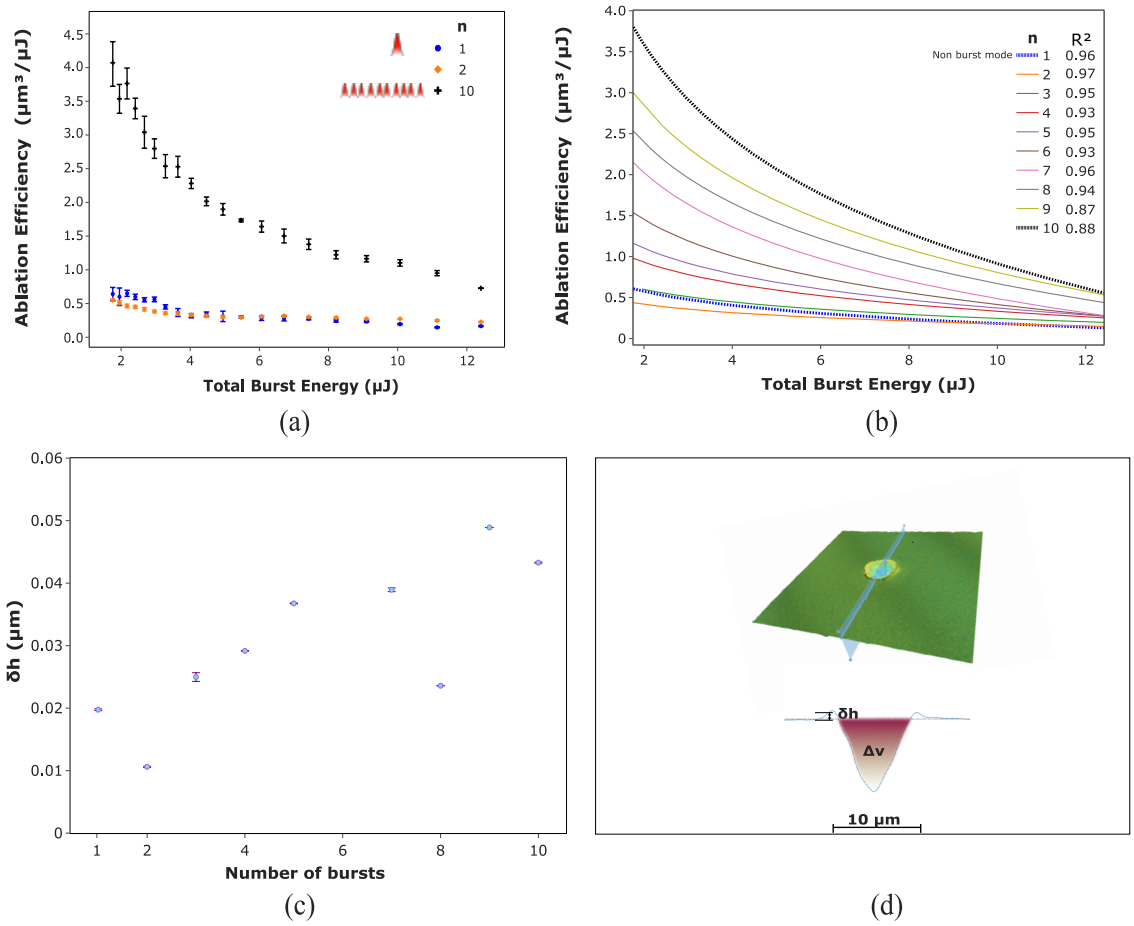

Fig. 2: (a) Experimental results for the ablation efficiency at different values of the total burst energy for n = 1 (NBM), 2 (PBM) and 10 (PBM). (b) Fit curves obtained from polynomial fits of the experimentally obtained ablation efficiency as a function of the total burst energy for different values of n. (c) Plot of the average burr height as a function of the number of pulses in a burst at E_{burst} = 10 μJ. (d) Top: Exemplary confocal profiler image and analysis plane through the spot center. Bottom: Two-dimensional representation of the analysis plane shown in the graph on the top.

The total burr height Δh obtained from the image analysis (see Fig. 2(d)) is also compared for different values of n.

Results and Discussion

Ablation efficiency. Fig. 2(a) shows experimental results for the ablation efficiency η at different values of the total burst energy for three different values of n. In accordance with the experimental results described in Refs. [3], [5], we observe an increase in material removal for higher values of n. The general behaviour is that, as the number of pulses in a burst is increased, the ablation efficiency is also increased. Compared to $n = 1$ (NBM), for n = 10 (PBM), the ablation efficiency increases by almost a factor of 10 for near ablation-threshold values of E_{burst} (≈1.4 μJ). The noticeable trend in ablation efficiency with respect to E_{burst} is not unexpected. The deeper the crater, the more laser fluence is required to keep the material removal at the same rate and, hence, a decrease in ablation efficiency is observed with an increase in E_{burst}. It may also be noted that η is lower for $n = 1$ compared to n = 2 (Fig. 2(a)). This observation could be explained in terms of the interaction of the second laser pulse in the burst with the ablated material. This second pulse may lead to re-deposition of material on the craters. This effect has previously been observed for all even numbered bursts [4]. However, for $n > 2$, we observe a steady increase in η (Fig. 2(b)).

At a given burst energy, the analysis of burr height values δh for different values of n reveals no significant trend (Fig. 3(c)). This is in contrast to previous observations by Matsumoto and co-workers [3] and could be explained by the different processing conditions. While our experiments are done with single bursts, the results by Matsumoto and co-workers were obtained after an accumulation of multiple bursts.

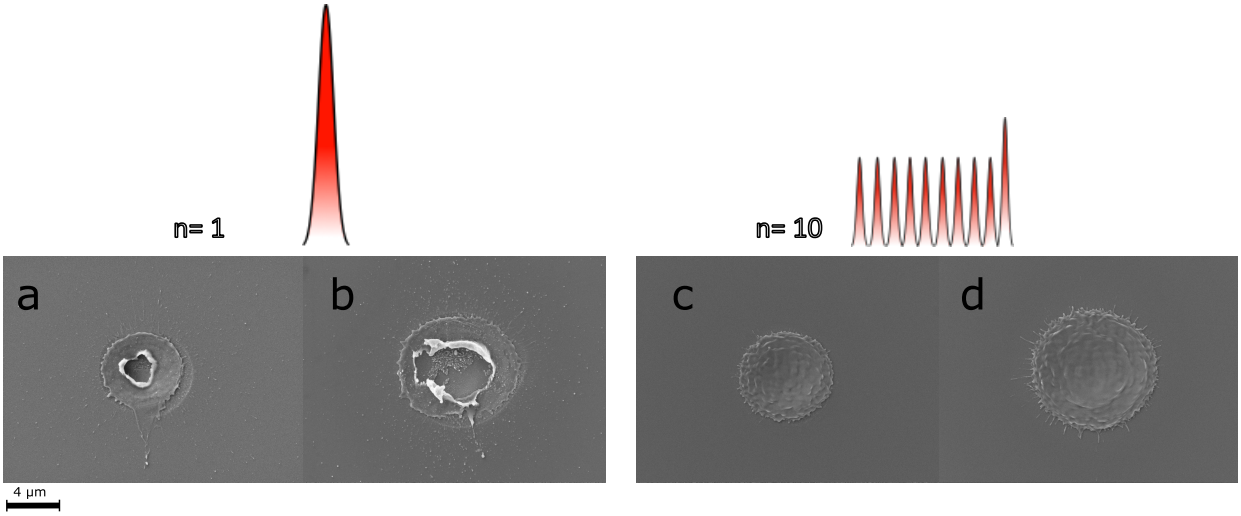

Fig. 3: SEM images of lasered craters obtained after laser micromachining under different processing conditions. (a) E_p = 3 μJ and n = 1, (b) E_p = 10 μJ and n = 1, (c) E_{burst} = 3 μJ and n = 10 and (d) E_{burst} = 10 μJ and n = 10

SEM. The SEM images in Fig. 3 clearly show a contrast in morphology between NBM and PBM. Figs. 3(a) and (b) show spots obtained using NBM (n = 1) with E_p = 3 μJ and 10 μJ, respectively. It is evident that, in NBM, high peak fluence leads to an increased roughness inside the lasered crater. Droplets of ejected particles are deposited around the circular ablated rim (Figs. 3 (a) and (b)). In contrast to that, the samples lasered using PBM appear to have a better surface quality. In Figs. 3(c) and (d), two examples are shown for which n = 10 and E_{burst} = 3 μJ and 10 μJ, respectively. The modifications show no evidence of ejected material around the crater. The theory of ablation cooling explained in Refs. [5] could be a plausible explanation for the observed improvement in the micromaching quality. The smoothness of craters (which is a general observation for all burst configurations) can also be explained as a signature of pulse bursts, due to the repetitive re-deposition of material inside the craters.

Summary and Conclusions

Our results show that, compared to the use of single fs laser pulses, GHz-burst fs laser micro-punching can lead to improved processing conditions for 4H-SiC. The resultant lowering of the thermal budget on the material following the controlled and repetitive removal of ablated material is a possible advantage of incorporating GHz pulse burst. 4H-SiC, as an indirect wide-bandgap material, could especially benefit from both the precision of fs laser pulses and the mitigation of unwanted nonlinear anomalies by the use of GHz bursts. While the present experiment reveals advantages for single burst surface modification, the same advantages can be expected for a variety of other laser manufacturing demands for 4H-SiC.

Acknowledgements

This work was supported by the Fraunhofer Society (Attract project ChemPyOn). H.M. also acknowledges support by the German Research Foundation (DFG; RTG 2717).

References

[1] B. Pecholt, S. Gupta, and P. Molian, "Review of laser microscale processing of silicon carbide," *Journal of Laser Applications*, vol. 23, no. 1, p. 012 008, 2011, ISSN: 1042-346X. DOI: 10.2351/1.3562522.

[2] C. Gaudiuso, P. N. Terekhin, A. Volpe, S. Nolte, B. Rethfeld, and A. Ancona, "Laser ablation of silicon with THz bursts of femtosecond pulses," *Scientific Reports*, vol. 11, no. 1, p. 13 321, 2021, ISSN: 20452322. DOI: 10.1038/s41598-021-92645-7.

[3] H. Matsumoto, Z. Lin, J. N. Schrauben, and J. Kleinert, "Ultrafast laser ablation of silicon with GHz bursts," *Journal of Laser Applications*, vol. 33, no. 3, p. 032 010, 2021, ISSN: 1042-346X. DOI: 10.2351/7.0000372.

[4] A. Žemaitis, M. Gaidys, P. Gečys, M. Barkauskas, and M. Gedvilas, "Femtosecond laser ablation by bibursts in the MHz and GHz pulse repetition rates," *Optics Express*, vol. 29, no. 5, p. 7641, 2021, ISSN: 10944087. DOI: 10.1364/oe.417883.

[5] C. Kerse, H. Kalaycloğ Lu, P. Elahi, *et al.*, "Ablation-cooled material removal with ultrafast bursts of pulses," *Nature*, vol. 537, no. 7618, pp. 84–88, 2016, ISSN: 14764687. DOI: 10.1038/nature18619.

[6] B. Neuenschwander, T. Kramer, B. Lauer, and B. Jaeggi, "Burst mode with ps- and fs-pulses: Influence on the removal rate, surface quality, and heat accumulation," *Laser Applications in Microelectronic and Optoelectronic Manufacturing (LAMOM) XX*, vol. 9350, no. March 2015, 93500U, 2015, ISSN: 1996756X. DOI: 10.1117/12.2076455.

[7] M. Sailer, F. Jansen, A. Fehrenbacher, *et al.*, "Optimized temporal energy deposition for advanced processing of Si and SiC based on highly flexible TruMicro series 2000," no. March 2021, p. 8, 2021, ISSN: 1996756X. DOI: 10.1117/12.2577590.

[8] N. Hodgson, H. Allegre, A. Starodoumov, and S. Bettencourt, "Femtosecond Laser Ablation in Burst Mode as a Function of Pulse Fluence and Intra-Burst Repetition Rate," *Journal of Laser Micro Nanoengineering*, vol. 15, no. 3, pp. 236–244, 2020, ISSN: 18800688. DOI: 10.2961/jlmn.2020.03.2014.